ACS APPLIED MATERIALS & INTERFACES

Research Article

www.acsami.org

Three-Dimensional Ordered ZnO/Cu_2O Nanoheterojunctions for Efficient Metal–Oxide Solar Cells

Xiang Chen,[†,§] Pei Lin,[†,§] Xiaoqin Yan,[†] Zhiming Bai,[†] Haoge Yuan,[†] Yanwei Shen,[†] Yichong Liu,[†] Guangjie Zhang,[†] Zheng Zhang,[†] and Yue Zhang*[,†,‡]

[†]State Key Laboratory for Advanced Metals and Materials, School of Materials Science and Engineering, University of Science and Technology Beijing, Beijing 100083, People's Republic of China

[‡]Key Laboratory of New Energy Materials and Technologies, University of Science and Technology Beijing, Beijing 100083, People's Republic of China

Supporting Information

ABSTRACT: Interface modulation for broad-band light trapping and efficient carrier collection has always been the research focus in solar cells, which provides the most effective way to achieve performance enhancement. In this work, solution-processed 3D ordered ZnO/Cu_2O nanoheterojunctions, consisting of patterned n-ZnO nanorod arrays (NRAs) and p-Cu_2O films, are elaborately designed and fabricated for the first time. By taking advantage of nanoheterojunctions with square patterned ZnO NRAs, solar cells demonstrate the maximum current density and efficiency of 9.89 mA cm^{-2} and 1.52%, which are improved by 201% and 127%, respectively, compared to that of cells without pattern. Experimental analysis and theoretical simulation confirm that this exciting result originates from a more efficient broad-band light trapping and carrier collection of the 3D ordered ZnO/Cu_2O nanoheterojunctions. Such 3D ordered nanostructures will have a great potential application for low-cost and all oxide solar energy conversion. Furthermore, the methodology applied in this work can be also generalized to rational design of other efficient nanodevices and nanosystems.

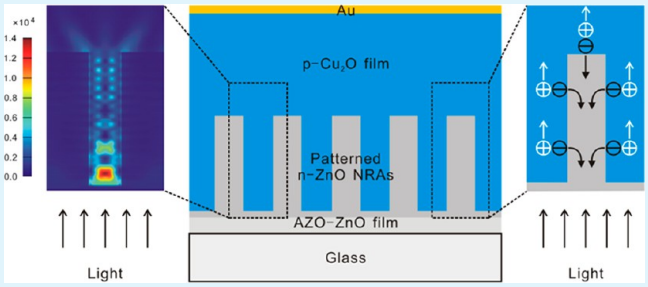

KEYWORDS: *laser interference lithography, 3D heterojunction, metal–oxide, solar cells, interface modulation*

INTRODUCTION

Efficient and reliable solar cells comprising earth-abundant and nontoxic metal–oxide absorbers are very attractive due to the sustainable material usage and potential for cost-effective manufacturing.[1] Cuprous oxide (Cu_2O), a natural p-type semiconductor with a direct band gap of ~2.0 eV, is one of the most promising candidates for solar energy conversion because of its theoretical power conversion efficiency of 20% and higher absorption coefficient than single-crystalline Si.[2] Doping Cu_2O to make it into stable n-type has proven to be challenging; thus, most research has been carried out by using n-ZnO/p-Cu_2O heterojunctions.[3−14] ZnO also has favorable characteristics for solar cell application, including its cost-effective, wide direct band gap (~3.37 eV) and high electron mobility (~120 cm^2 V s^{-1}).[10] Overall, both materials are inexpensive, abundant, and photon stable.[11] Despite these advantages, the cell efficiency in practice remains low, achieving 4.12% with Cu_2O sheet fabricated by thermal oxidation (TO) at 1010 °C and only 1.43% with Cu_2O thin film via electrochemical deposition (ECD) at 65 °C, respectively.[13,14] Poor light harvesting capability and low carrier collection efficiency are two of the most common issues in such 2D ZnO/Cu_2O heterojunctions.[11,12,15]

To address this issue, 3D ZnO/Cu_2O nanoheterojunctions, assembled with ZnO nanorod arrays (NRAs) and Cu_2O films, are preferred to be used recently.[16−24] For example, Cui's group reported that a 60% efficiency improvement was achieved by using 3D ZnO/Cu_2O nanoheterojunctions instead of 2D ones.[16] This report, together with many others, suggests that increasing the heterojunction area, together with high crystallinity of ZnO and Cu_2O layers, is the most important way to obtain large current densities for such solar cells.[17,18,24] However, the ZnO NRAs applied in most of the research have random orientation and arrangement, which will not only jeopardize the heterointerface property and film crystallinity but also increase carrier recombination.[18,25] Therefore, vertically aligned highly ordered ZnO NRAs with good crystallinity and uniform distribution are required for such efficient metal–oxide solar cells.

As we know, the efficiency of a solar cell depends on the probability of an incident photon being absorbed and then collection of generated carriers, that is, broad-band light

Received: November 10, 2014
Accepted: January 16, 2015
Published: January 16, 2015

DOI: 10.1021/am507836v
ACS Appl. Mater. Interfaces 2015, 7, 3216−3223

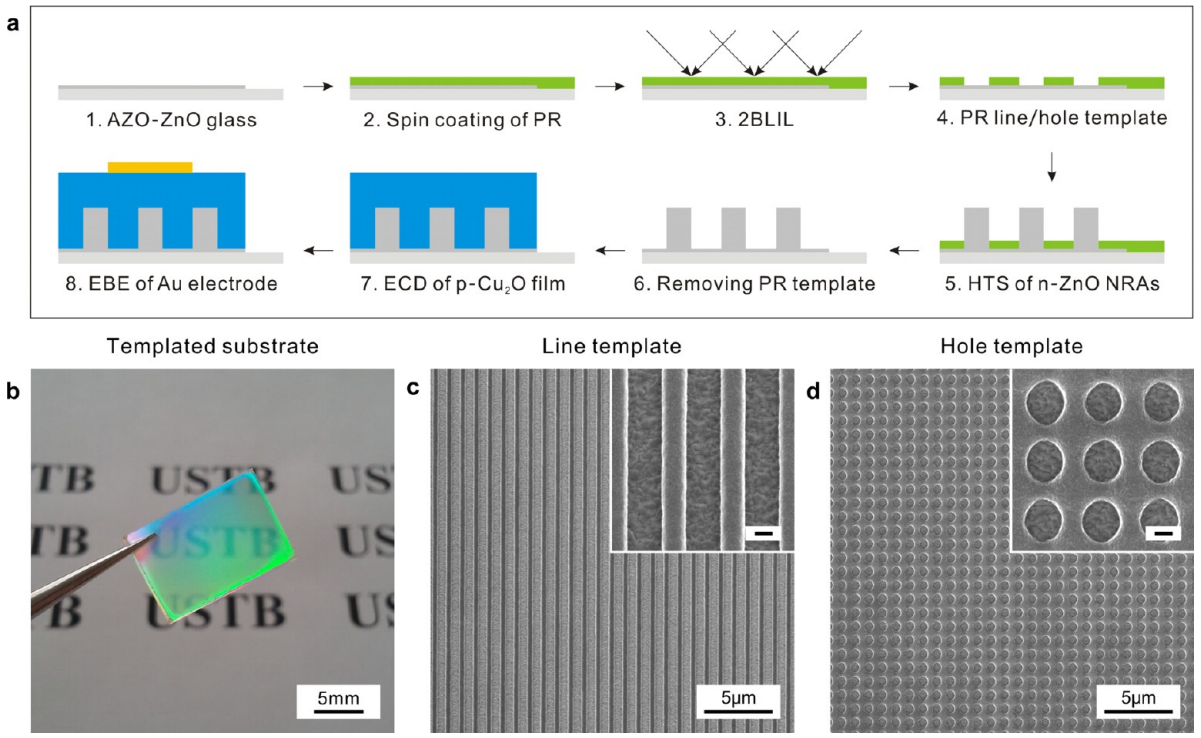

Figure 1. (a) Schematic illustration of the fabrication sequence of metal−oxide solar cells with 3D ordered ZnO/Cu_2O nanoheterojunction via 2BLIL, HTS, and ECD. (b) Optical image of an AZO-ZnO glass covered with large-scale patterned PR template. (c and d) Top view SEM images of the PR line (c) and hole (d) templates in a period of 1 μm with uniform distribution. (Insets) Corresponding magnified SEM images; scale bars are 300 nm.

absorption and ultralow reflectivity are needed first and foremost.[1] In the past few years, 3D ordered nanostructures have been widely used in Si,[26−29] GaAs,[30,31] polymer,[32,33] and dye-sensitized[34,35] solar cells to achieve absorption enhancement and reflection reduction. For instance, Fan's group demonstrated that properly designed 3D ordered Si nanowell arrays can serve as a broad-band and efficient photon harvester.[26] Huffaker's group reported a 3D ordered core−shell organic−inorganic hybrid solar cell with an improved short-circuit current density (J_{sc}) and power conversion efficiency (η) of 13.6 mA cm^{-2} and 4.11%.[30] Besides enhancing light absorption, the 3D ordered nanostructures can also promote carrier collection significantly if the nanostructures are properly designed.[1,29,33] If, for example, the p−n junction interface is parallel to the light absorption direction, carriers can be collected perpendicularly to the absorption direction.[33] Such structures will significantly decrease the traveling distance for carriers and thus reduce the loss of electrons from recombination.[36,37] However, the facile fabrication of 3D ordered ZnO/Cu_2O nanoheterojunctions and their effects on the performance of solar cells have rarely been reported so far. There are also few reports focusing on the realization of broad-band light trapping and efficient carrier collection simultaneity in such all metal−oxide solar cells.

Herein, we report our efforts into fabrication of the first 3D ordered ZnO/Cu_2O nanoheterojunction solar cells, assembled with periodically patterned ZnO NRAs and electrodeposited Cu_2O film. First, elaborate design of ZnO NRAs with different density and morphology was achieved by using two-beam laser interference lithography (2BLIL) and a hydrothermal synthesis (HTS) method.[38−42] Next, the remarkable influence of length, arrangement, and density of patterned ZnO NRAs on the performance of this Cu_2O/ZnO solar cell was systematically investigated. By using square patterned ZnO NRAs, cells demonstrated the best efficiency and theoretical simulations confirmed that this improvement is primarily attributed to broad-band light trapping and efficient carrier collection of such 3D ordered nanoheterojunctions. Overall, this study presents an effective approach to arbitrarily control the incident light in metal−oxide solar cells which could be extended to other nanodevices and nanosystems design.

EXPERIMENTAL SECTION

Fabrication of patterned photoresist templates via 2BLIL starts with the deposition of AZO-ZnO films (AZO ≈ 900 nm, resistance ≤ 10 Ω sq^{-1}, transmittance ≥ 80%; ZnO ≈ 50 nm) first and successively on float glass with the radiofrequency magnetron sputtering method. As growing substrate, the conductive AZO-ZnO glass was cut into small pieces with dimensions of 15 mm × 10 mm, ultrasonically cleaned in acetone, isopropyl alcohol (IPA), and deionized water each for 5 min, and blow dried gently with N_2 gas. Second, negative photoresist (PR) AR-N 4340 (Allresist GmbH) diluted with thinner AR 300−12 (1:1 weight ratio) was spin coated on the substrate at a speed of 4000 rpm for 30 s to form a uniform PR layer (~400 nm), which was followed by a soft baking process at 85 °C on a hot plate for 2 min. Third, the PR-coated substrates were exposed by 2BLIL using a self-designed lithography system (Supporting Information, Figure S1a).[39] In this system, all optical components were placed into a closed plexiglass cabinet to avoid the formation of low-contrast PR templates, which will be caused by thermal or air disturbance.[40] In this research, two exposure modes were employed (single exposure at 0° for 80 s and double exposure at 0° + 90° for 2 × 35 s). Finally, the substrates were postbaked at 95 °C on a hot plate for 80 s, developed in AR 300−475 and deionized water mixed solution (1:1 volume ratio) for 6 min, rinsed with deionized water for 30 s and blow dried using N_2 gas to obtain PR line and hole templates on AZO-ZnO substrates.

DOI: 10.1021/am507836v
ACS Appl. Mater. Interfaces 2015, 7, 3216−3223

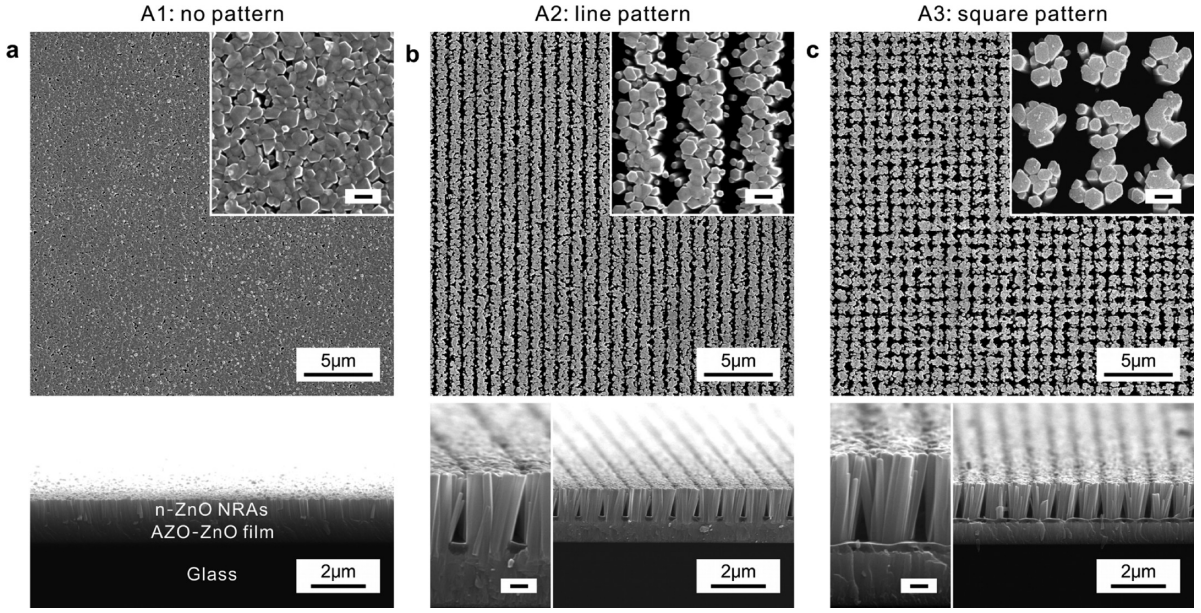

Figure 2. Top and cross-sectional SEM images of the ZnO NRAs with no pattern (a), line pattern (b), and square pattern (c) (named A1, A2, and A3, respectively). Patterned ZnO NRAs were obtained by using the PR line and hole templates. The growth time of each ZnO NRAs was 3 h. (Insets) Corresponding magnified SEM images; scale bars are 300 nm.

Synthesis of patterned n-ZnO NRAs was accomplished via a chemical bath deposition method on the above patterned AZO-ZnO substrates. The precursor aqueous solution contains equal molar zinc nitrate and hexamethylenetetramine with a concentration of 0.05 mol L^{-1}, and the growth was conducted at 95 °C for 3 h. During this process small bubbles may be produced in aqueous solution, partially cover the surface of substrates, and stop the growth of ZnO NRAs at that position. To overcome this bubble effect, the substrates were nipped in the solution by corrosion-resistant alligator clips; thus, the reaction container could be knocked periodically to remove the bubbles inside as well as no influence on the overall reaction (see Figure S1b, Supporting Information). Then the substrates were cleaned by rinsing with PR remover AR 300−72 for 30 s, deionized water for 30 s, and IPA for 1 min and dried in an oven at 60 °C for 15 min. An oxygen-plasma treatment (O_2 300 sccm, 100 W, 60 s) was further employed to remove any residual PR particles and clean the surface of patterned ZnO NRAs. After that, p-Cu_2O films were cathodically deposited onto the ZnO NRAs using an aqueous solution containing 0.4 mol L^{-1} copper sulfate and 3 mol L^{-1} lactic acid that was adjusted to pH 12.5 with 4 mol L^{-1} sodium hydroxide solution. The deposition was carried out galvanostatically in a three-electrode system under −1.0 mA cm^{-2} for 30 min at 40 °C. The reference electrode was standard saturated Ag/AgCl electrode, and a Pt sheet serves as counter electrode. Afterward, the substrates were rinsed with deionized water and blow dried using N_2 gas. Last, a thin gold layer (~100 nm) was evaporated onto the Cu_2O film by electron-beam evaporation as the top electrode. For comparison, no patterned ZnO NRAs (without using PR template during HTS process) were also applied to fabricate the metal−oxide solar cells in this study.

The morphological investigations of PR templates, ZnO NRAs, and ZnO/Cu_2O heterojunctions were conducted by field emission scanning electron microscopy (FESEM, FEI QUANTA 3D). The crystal structure and orientation of the ZnO NRAs and Cu_2O films were investigated by X-ray diffraction (XRD, Rigaku DMAX-RB, Cu Kα). UV−vis−NIR absorption of the NRAs and heterojunctions were also investigated using a UV−vis−NIR spectrophotometer (Varian Cary 5000). The current−voltage (J−V) characteristics of this metal−oxide solar cells were measured with electrochemical workstation (Solartron SI 1287/SI 1260) under AM 1.5G illumination provided by a solar simulator (Oriel, 91159A, 100 mW cm^{-2}). The external quantum efficiency (EQE) measurements were carried out using Qtest Station 500ADI calibrated by a Si photodetector (CROWNTECH).

RESULTS AND DISCUSSION

A flowchart of the ZnO/Cu_2O solar cell fabrication process is schematically presented in Figure 1a. Figure 1b shows the optical image of large-scale patterned photoresist (PR) templates on AZO-ZnO substrates. The colorful AZO-ZnO glass indicates that periodical PR template has covered the whole surface, which benefits the realization of patterned ZnO NRAs with a uniform distribution. In addition, using single and double exposures, PR line and hole templates in a period of 1 μm were both obtained, as indicated in Figure 1c and 1d.[38,39] These two PR templates were employed to define the nucleation site, period, and arrangement of patterned ZnO NRAs later in this study.

Optical pictures of the fabricated three kinds of ZnO NRAs (with no pattern, line and square patterns) are presented in Figure S2a, Supporting Information, while corresponding top-view and cross-sectional SEM images are shown in Figure 2a−c. The first, named A1, was prepared without using PR template. The second and third, named A2 and A3, were obtained with the help of PR line and hole templates. It is clear that all ZnO NRAs are uniformly distributed in a large area (nanorod diameter ≈ 200 nm) and vertically aligned due to the high-quality AZO-ZnO films used in this research. The differences between A1−A3 are shown in the arrangement, density, and length of the ZnO NRAs. A1 has a dense ZnO NRAs without arrangement the maximum density ≈ 3.8×10^9 rod cm^{-2} and minimum length ≈ 1 μm. In contrast, under the influence of PR templates, the nucleation and growth of ZnO NRAs can only be achieved where the AZO-ZnO films at the bottom are exposed. Therefore, a line template produces ZnO NRAs with a line pattern (period 1 μm, density ≈ 2.7×10^9 rod cm^{-2}, length ≈ 1.5 μm), and a hole template leads to ZnO NRAs with a square pattern (period 1 μm, density ≈ 1.2×10^9 rod cm^{-2}, length ≈ 2 μm). Multiple ZnO NRAs grow out of each line and hole because the PR space are so wide that lots of small ZnO grains were exposed.[38] Note that all of the growth solution concentration is fixed at 0.05 mol L^{-1}; thus, the smaller the

DOI: 10.1021/am507836v
ACS Appl. Mater. Interfaces 2015, 7, 3216−3223

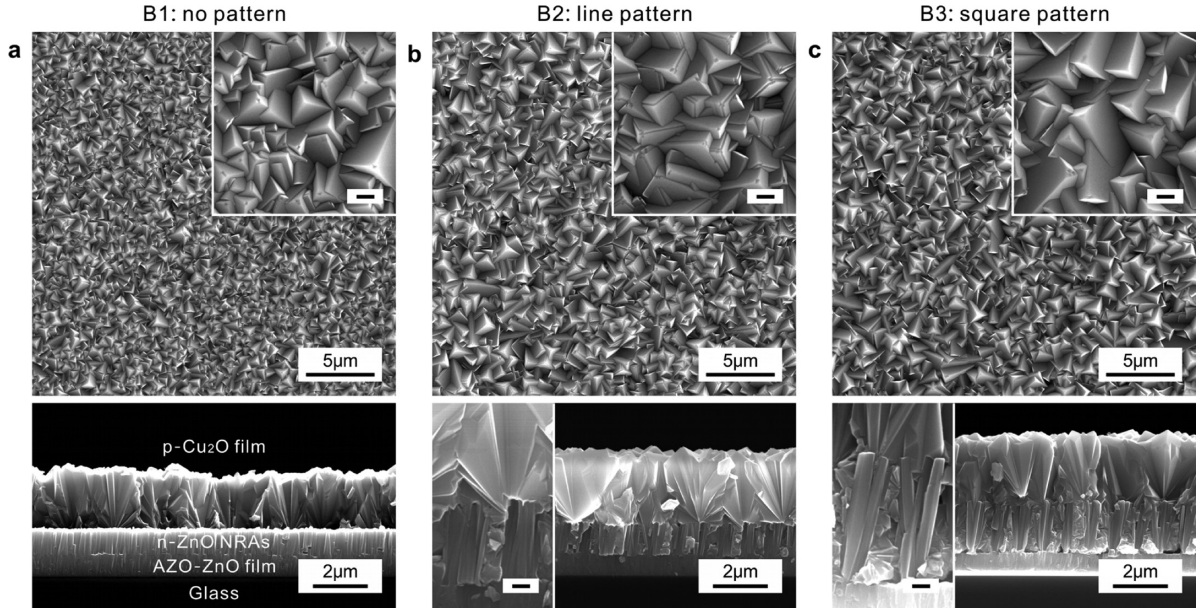

Figure 3. Top and cross-sectional SEM images of the ZnO/Cu_2O heterojunctions based on the ZnO NRAs with no pattern (a), line pattern (b), and square pattern (c) (named B1, B2, and B3, respectively). The deposition time of each Cu_2O film was 30 min. (Insets) Corresponding magnified SEM images; scale bars are 300 nm.

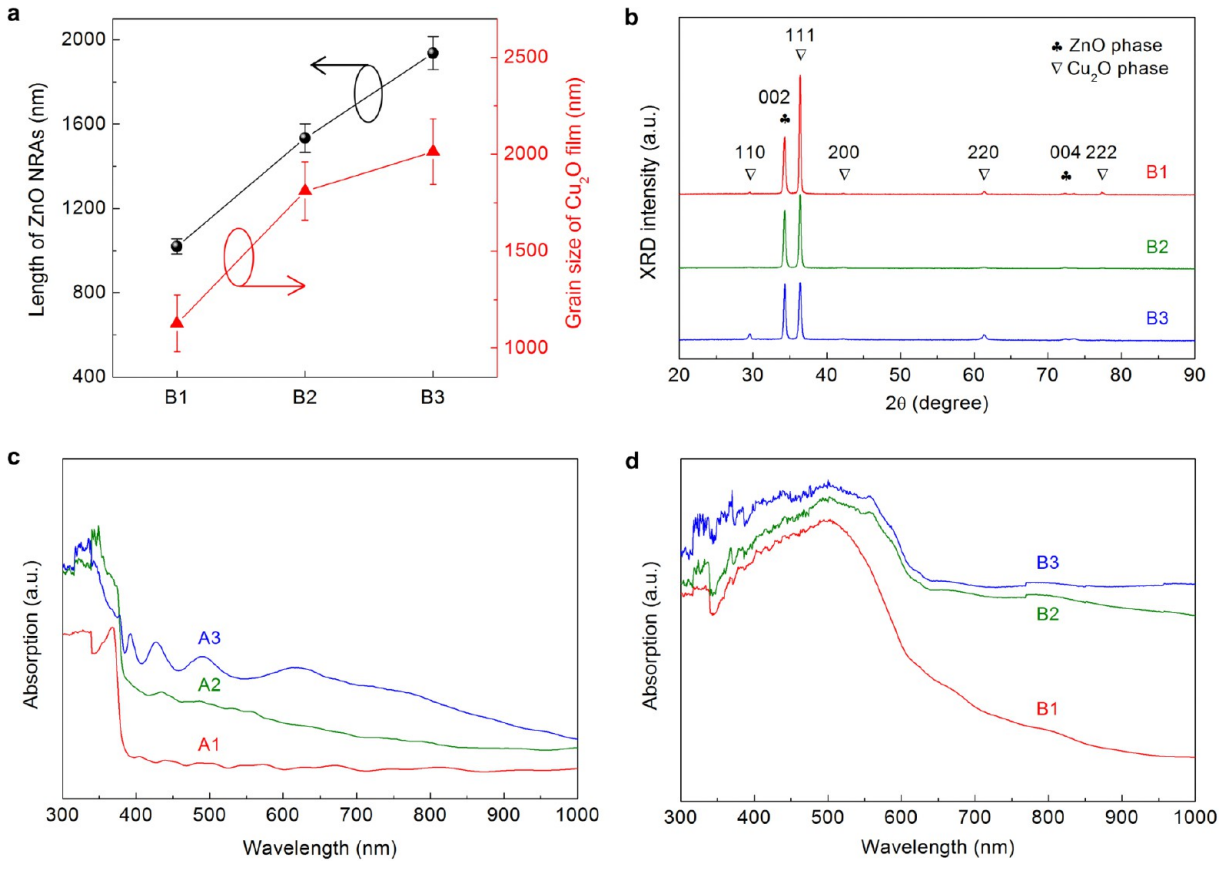

Figure 4. (a) Length of the ZnO NRAs and grain size of the Cu_2O film in each heterojunction from B1 to B3. (b) XRD results of B1−B3. (c) UV−vis−NIR absorption spectra of the ZnO NRAs with and without pattern from A1 to A3. (d) UV−vis−NIR absorption spectra of B1−B3.

areas exposed, the more precursor nutrition will be gained for nanorods in per unit area. That is why the ZnO NRAs with a square pattern have the longest length.

Three kinds of ZnO/Cu_2O heterojunctions were prepared by electrochemically depositing p-Cu_2O films onto the n-ZnO NRAs shown above. The corresponding optical pictures are also presented (Figure S2b, Supporting Information). The first, named B1, has a 2D ZnO/Cu_2O heterojunction, as presented in Figure 3a. The second and third, named B2 and B3, have 3D ordered ZnO/Cu_2O nanoheterojunctions, as shown in Figure

DOI: 10.1021/am507836v
ACS Appl. Mater. Interfaces 2015, 7, 3216−3223

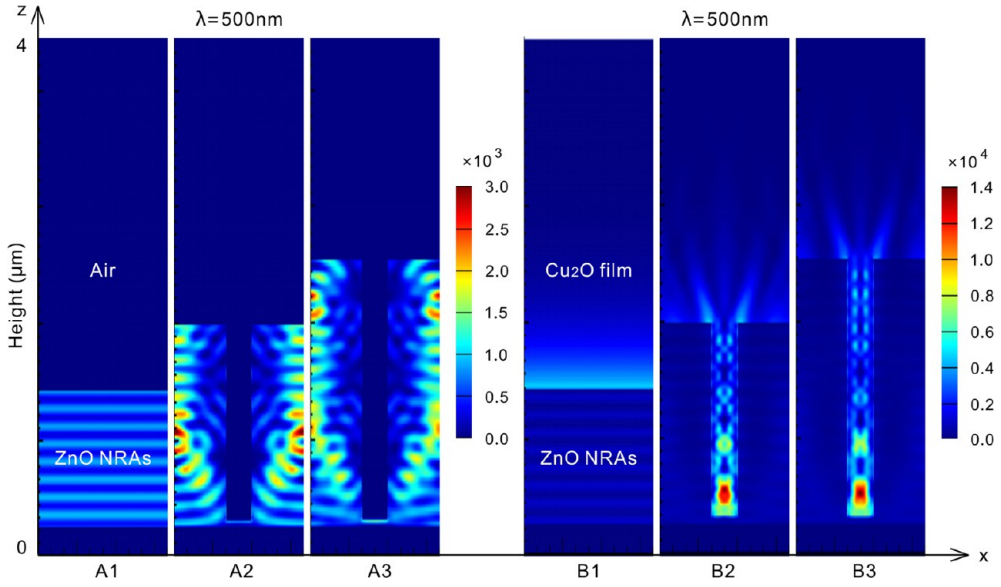

Figure 5. Simulated cross-sectional optical absorption profiles in different ZnO NRAs (A1−A3) and ZnO/Cu_2O heterojunctions (B1−B3), illuminated with a planar light from the bottom (λ = 500 nm).

3b and 3c. Obviously, all of the Cu_2O films are composed of pyramid grains grown in the direction normal to the substrate surface. The pyramid-like textured surface helps increase the light path and facilitate photons to be absorbed more effectively in the solar cells.[4,12,20,24] No obvious defects, such as pores or pinholes, are observed on the surface and throughout the film thickness. Such dense and continuous films will avoid the direct contact between Au and ZnO and help reduce leakage current of the solar cells.[7,15,19] Besides, the films in B2 and B3 completely fill the ordered spaces among patterned ZnO NRAs, forming true 3D ordered ZnO/Cu_2O nanoheterojunctions. The differences between B1 and B3 are shown in the grain size, thickness, and heterojunction area of the Cu_2O films. As the length of ZnO NRAs in B1−B3 changes from ∼1 to ∼2 μm, the grain size of Cu_2O becomes larger from ∼1.1 to ∼1.8 to ∼2 μm, as indicated in Figure 4a, the thickness is increased from ∼2.2 to ∼3.7 to ∼4.2 μm, and the heterojunction area is enlarged from 1 to ∼3.9 to ∼5.2 cm^2 (Figure S3a, Supporting Information). The large Cu_2O grains, caused by fewer nucleation sites on the top surface of the patterned ZnO NRAs, are promising for photovoltaic applications because of the reduction of recombination probability at grain boundaries.[6,9,11,36] In addition, the thick films and large heterojunction areas, due to the patterned ZnO NRAs with increased length and surface area, are beneficial for promoting the generation and separation of excitons in solar cells.[16,17,21]

Moreover, the crystal structures and light absorption properties of the ZnO NRAs and ZnO/Cu_2O heterojunctions were investigated. First, the XRD pattern for pure ZnO NRAs (A1) shows only two main peaks at 34.45° and 72.56°, corresponding to the ZnO (002) and (004) planes (Figure S3b, Supporting Information). It indicates that the ZnO NRAs are highly *c*-axis oriented, which will induce the growth of Cu_2O crystals with preferential ⟨111⟩ orientation and lead to a good crystallographic matching.[8,19] Hence, the XRD pattern for ZnO/Cu_2O heterojunction (B2) contains not only the diffraction peaks of ZnO but also many diffraction peaks of Cu_2O, especially the strong one to the (111) plane. On the basis of this good crystallographic matching, formation of interface states during the heterojunction epitaxial growth can be restrained, which will effectively limit the recombination of electrons in n-ZnO with holes in p-Cu_2O at the interface region and enhance the built-in potential.[11,15,18,22] Second, It can be perceived that the intensity of the Cu_2O (111) peak for B1−B3 is decreased gradually relative to the ZnO (002) peak, as shown in Figure 4b, that is it may be attributed to the increased length and surface area of the patterned ZnO NRAs.[21] Even so, these Cu_2O (111) peaks have higher intensities, which indicates that the ZnO/Cu_2O heterojunctions in this work have improved crystal qualities.[3,19,23,24] Third, due to the effect of strong light scattering (Figure S2a, Supporting Information), the patterned ZnO NRAs present wide absorbance bands rather than the no patterned one, and A3 demonstrates the highest absorption of the three tested samples, as indicated in Figure 4c. Meanwhile, their transmission spectra are just the opposite (Figure S3c, Supporting Information). Note that A3 has a slightly reduced absorption in the UV region relative to A2, which may result from the decreased density of ZnO NRAs. Finally, the light scattering from patterned ZnO NRAs will not only increase with nanorod length but also result in an enhancement of the optical path length and absorption in a surrounding material.[1,35] Therefore, the 3D ordered ZnO/Cu_2O nanoheterojunctions show enhanced and broad-band light trapping capabilities, especially when the wavelength is larger than 500 nm, and B3 has the maximum absorption and the minimum transmission of the three tested samples (Figure 4d; Figure S3d, Supporting Information).

To further understand the light absorption in the ZnO NRAs and ZnO/Cu_2O heterojunctions, two-dimensional finite difference time domain (FDTD) simulations were performed (Lumerical FDTD solutions 8.6), as shown in Figure 5. Three kinds of simulation models were established by reference to the length (1, 1.5, and 2 μm) and space (0, 200, and 200 nm) of the ZnO NRAs (Figure S4, Supporting Information). When the top layers were defined as air or Cu_2O, the models were corresponding to A1−A3 or B1−B3, respectively.[15,26] The simulated regions were 1 μm × 4 μm in size, with periodic boundary conditions in the *x* direction and perfectly matched layer (PML) boundary conditions in the *z* direction. Besides, the models were illuminated with a plane wave from the AZO

DOI: 10.1021/am507836v
ACS Appl. Mater. Interfaces 2015, 7, 3216−3223

Table 1. Comparison of Photovoltaic Properties of the Metal−Oxide Solar Cells[a]

cells	ZnO NRAs	V_{oc} (V)	J_{sc} (mA/cm^2)	FF	η (%)
B1	no pattern	0.49 ± 0.01	3.29 ± 0.08	0.42 ± 0.02	0.67 ± 0.10
B2	line pattern	0.44 ± 0.02	7.76 ± 0.06	0.39 ± 0.03	1.34 ± 0.14
B3	square pattern	0.42 ± 0.02	9.89 ± 0.13	0.37 ± 0.04	1.52 ± 0.12

[a]Measurements were performed under 1 sun illumination (AM 1.5G, light intensity 100 mW/cm^2). The active areas were ~0.25 cm^2 for all of the cells, and the data presented are average values obtained after testing 10 cells.

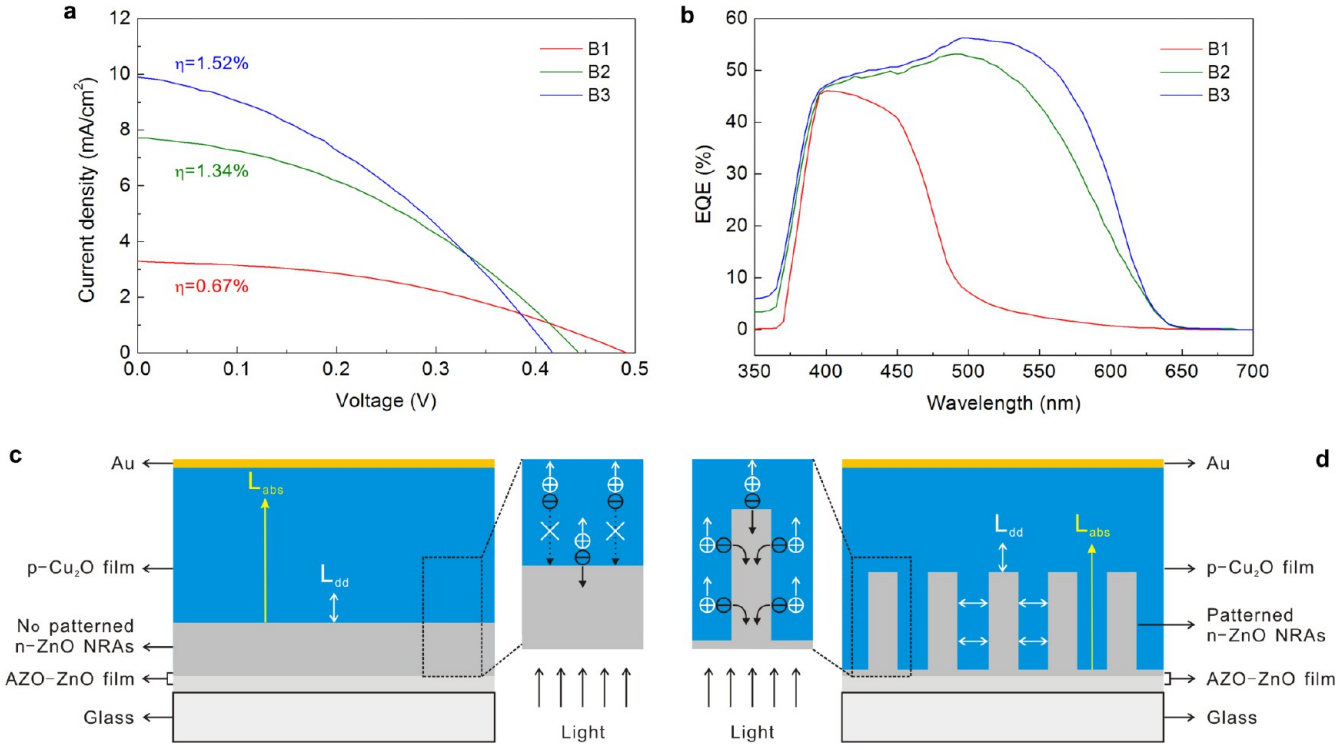

Figure 6. (a and b) J−V curves (a) and EQE spectra (b) of the metal−oxide solar cells based on the ZnO/Cu_2O heterojunctions from B1 to B3. (c and d) Schematics of the metal−oxide solar cells with ZnO/Cu_2O 2D heterojunction (c) and 3D ordered nanoheterojunction (d).

side, and the simulation was run long enough to reach steady state. To reveal the propagation nature of a plane light in A1−A3 and B1−B3, taking λ = 500 nm as an example, the simulated electric-field intensity |E| distributions are visualized (Figure S5, Supporting Information). It is clear that that |E| has been enhanced in some ZnO areas (A2−A3) and Cu_2O areas (B2−B3) when under the influence of periodic ZnO NRAs coupling with light reflection and interference.[26,27] Accordingly, the light absorption in such areas are enhanced, and more enhancements will be achieved if the ZnO NRAs have longer length and square pattern (periodically in both x and y directions). These results are well coincident with the absorption spectra shown Figure 4. Note that the |E| and absorption enhancements, caused by the 3D ordered ZnO/Cu_2O nanoheterojunctions, will be more apparent when the wavelength of the light is larger than 500 nm (Figure S6, Supporting Information). That is why B2−B3 have broad-band light trapping capabilities. Besides, such capability will be further improved by enlarging the space between two adjacent nanorods, because more Cu_2O can be filled into the space (Figure S7, Supporting Information). For these reasons, B3 achieves the highest absorption among B1−B3. In general, both experimental and simulation results suggest that the 3D ordered ZnO/Cu_2O nanoheterojunctions with square patterned ZnO NRAs are best suited for realizing broad-band and efficient light trapping in metal−oxide solar cells.

The photoelectric characteristics of the solar cells, such as open-circuit voltage (V_{oc}), short-circuit current density (J_{sc}), fill factor (FF), and power conversion efficiency (η), are summarized in Table 1. The solar cell based on B1 exhibited a V_{oc} of 0.49 V, J_{sc} of 3.29 mA cm^{-2}, FF of 0.42, and η of 0.67%. By replacing B1 with B2 and B3, the J_{sc} and η of the solar cells were improved gradually, as shown in Figure 6a. The solar cell based on B3 exhibited a maximum efficiency of 1.52% (V_{oc} of 0.42 V, J_{sc} of 9.89 mA cm^{-2}, and FF of 0.37), which is 2.3 times higher than that of the reference cell B1. It can be seen that smaller V_{oc} and FF were achieved from patterned solar cells compared with that of no patterned ones. We attributed this phenomena to increased heterointerface area for 3D Cu_2O/ZnO junction, which decreased the internal impedance.[16,18] However, the J_{sc} increased more dramatically; thus. the overall efficiency was enhanced.

To gain insight on the origin of the J_{sc} and η increments, EQE measurements were also performed, as presented in Figure 6b. Compared with B1, the values of EQE for the solar cells with B2−B3 increase significantly when λ > 380 nm, reaching the maximums when λ = 490 nm, and decrease gradually when λ > 490 nm. The EQE profiles agree well with the absorption spectra of B1−B3, which indicates that the improvements on J_{sc} and η are largely attributed to the broad-band and efficient light absorption of B2−B3, which can

DOI: 10.1021/am507836v
ACS Appl. Mater. Interfaces 2015, 7, 3216−3223

produce greater amounts of excitons in the active layers.[12,22] Furthermore, as we know, light absorption and photocarrier collection are in conflict for 2D heterojunction solar cells.[1,33] Paths of the photon and the minority carrier are in the same direction and carriers cannot be collected effectively where photon absorption length (L_{abs}) is larger than minority carrier drift-diffusion length (L_{dd}), as shown in Figure 6c.[17,36,37] In particular, this effect is more evident for electrodeposited Cu_2O because it has a shorter minority drift-diffusion length compared with thermally oxidized Cu_2O.[43,44] That is why the EQE of the solar cell with B1 is decreased when $\lambda > 380$ nm, which is similar to the one presented in previous works.[6,11,12,15] By contrast, 3D ordered nanoheterojunctions with patterned ZnO NRAs can greatly reduce the conflict between light absorption and carrier collection, especially for long wavelength photons, since the heterointerface is parallel to the light absorption direction and carriers can be collected perpendicularly to the absorption direction, as indicated in Figure 6d. Besides, the Cu_2O that grows inside adjacent ZnO nanorods is fully depleted, facilitating the carriers transport in it. Such structures significantly decrease the traveling distance for carriers and reduce the loss of electrons from recombination.[17,33,36]

Above all, the J_{sc} and η increments are attributed to not only the broad-band light trapping but also the efficient carrier collection. In this case, 3D ordered ZnO/Cu_2O nanoheterojunction with square patterned ZnO NRAs is the best choice for the realization of efficient metal−oxide solar cells.

CONCLUSION

In summary, this work demonstrates an effective approach to fabricate 3D ordered ZnO/Cu_2O nanoheterojunctions in order to boost the efficiency of related metal−oxide solar cells. By using the nanoheterojunctions with square patterned ZnO NRAs, the cells achieve the maximum current density and efficiency of 9.89 mA cm^{-2} and 1.52%, which are improved by 201% and 127% compared to the reference cells with no patterned ZnO NRAs. This improvement is attributed to broad-band light trapping capability and high carrier collection efficiency of the 3D ordered nanoheterojunctions. Furthermore, the results reveal that optimization of material and interface qualities, as well as device geometry, will be an important next step toward achieving higher efficiencies. This research opens up a new design and exciting opportunity for low-cost metal−oxide solar cells to control, confine, and utilize the incident light more effectively, which could be extended to many other nanodevices and nanosystems.

ASSOCIATED CONTENT

Supporting Information

Details on the following topics: optical images of 2BLIL system, HTS reaction container and three kinds of ZnO NRAs before and after Cu_2O film deposition, UV−vis−NIR transmission spectra of A1−B3, schematics of the FDTD simulation models, simulated cross-sectional electric-field intensity distributions in A1−B3 and B3 with light wavelength from 350 to 600 nm, simulated cross-sectional optical absorption profiles in B3 with distance from 100 to 800 nm between two adjacent nanorods. This material is available free of charge via the Internet at http://pubs.acs.org.

AUTHOR INFORMATION

Corresponding Author

*Tel.:+86-010-62332011. E-mail: yuezhang@ustb.edu.cn.

Author Contributions

§These two authors contributed equally to this work.

Notes

The authors declare no competing financial interest.

ACKNOWLEDGMENTS

This work was supported by the National Major Research Program of China (2013CB932602), the Major Project of International Cooperation and Exchanges (2012DFA50990), the Program of Introducing Talents of Discipline to Universities, NSFC (51232001, 51172022, 51372023, 51372020), the Research Fund of Co-construction Program from Beijing Municipal Commission of Education, the Fundamental Research Funds for the Central Universities, the Program for Changjiang Scholars, and the Innovative Research Team in University.

REFERENCES

(1) Yu, M.; Long, Y.-Z.; Sun, B.; Fan, Z. Recent Advances in Solar Cells Based on One-Dimensional Nanostructure Arrays. *Nanoscale* **2012**, *4*, 2783−2796.

(2) Rühle, S.; Anderson, A. Y.; Barad, H.-N.; Kupfer, B.; Bouhadana, Y.; Rosh-Hodesh, E.; Zaban, A. All-Oxide Photovoltaics. *J. Phys. Chem. Lett.* **2012**, *3*, 3755−3764.

(3) Chen, L.-C. Review of Preparation and Optoelectronic Characteristics of Cu_2O-Based Solar Cells with Nanostructure. *Mater. Sci. Semicond. Proc.* **2013**, *16*, 1172−1185.

(4) Wei, H. M.; Gong, H. B.; Chen, L.; Zi, M.; Cao, B. Q. Photovoltaic Efficiency Enhancement of Cu_2O Solar Cells Achieved by Controlling Homojunction Orientation and Surface Microstructure. *J. Phys. Chem. C* **2012**, *116*, 10510−10515.

(5) McShane, C. M.; Choi, K.-S. Junction Studies on Electrochemically Fabricated p-n Cu_2O Homojunction Solar Cells for Efficiency Enhancement. *Phys. Chem. Chem. Phys.* **2012**, *14*, 6112−6118.

(6) Mittiga, A.; Salza, E.; Sarto, F.; Tucci, M.; Vasanthi, R. Heterojunction Solar Cell with 2% Efficiency Based on a Cu_2O Substrate. *Appl. Phys. Lett.* **2006**, *88*, 163502.

(7) Masanobu, I.; Tsutomu, S.; Ko-Taro, M.; Yuya, I.; Minoru, I.; Akimasa, T. Electrochemically Constructed p-Cu_2O/n-ZnO Heterojunction Diode for Photovoltaic Device. *J. Phys. D Appl. Phys.* **2007**, *40*, 3326.

(8) Jeong, S. S.; Mittiga, A.; Salza, E.; Masci, A.; Passerini, S. Electrodeposited ZnO/Cu_2O Heterojunction Solar Cells. *Electrochim. Acta* **2008**, *53*, 2226−2231.

(9) Septina, W.; Ikeda, S.; Khan, M. A.; Hirai, T.; Harada, T.; Matsumura, M.; Peter, L. M. Potentiostatic Electrodeposition of Cuprous Oxide Thin Films for Photovoltaic Applications. *Electrochim. Acta* **2011**, *56*, 4882−4888.

(10) Duan, Z.; Du Pasquier, A.; Lu, Y.; Xu, Y.; Garfunkel, E. Effects of Mg Composition on Open Circuit Voltage of Cu_2O−$Mg_xZn_{1-x}O$ Heterojunction Solar Cells. *Sol. Energy Mater. Sol. Cells* **2012**, *96*, 292−297.

(11) Zoolfakar, A. S.; Rani, R. A.; Morfa, A. J.; Balendhran, S.; O'Mullane, A. P.; Zhuiykov, S.; Kalantar-zadeh, K. Enhancing the Current Density of Electrodeposited ZnO-Cu_2O Solar Cells by Engineering Their Heterointerfaces. *J. Mater. Chem.* **2012**, *22*, 21767−21775.

(12) Marin, A. T.; Muñoz-Rojas, D.; Iza, D. C.; Gershon, T.; Musselman, K. P.; MacManus-Driscoll, J. L. Novel Atmospheric Growth Technique to Improve Both Light Absorption and Charge Collection in ZnO/Cu_2O Thin Film Solar Cells. *Adv. Funct. Mater.* **2013**, *23*, 3413−3419.

DOI: 10.1021/am507836v
ACS Appl. Mater. Interfaces 2015, 7, 3216−3223

(13) Nishi, Y.; Miyata, T.; Minami, T. The Impact of Heterojunction Formation Temperature on Obtainable Conversion Efficiency in n-ZnO/p-Cu_2O Solar Cells. *Thin Solid Films* **2013**, *528*, 72−76.
(14) Kazuya, F.; Takeo, O.; Tsuyoshi, A. Fabrication and Characterization of ZnO/Cu_2O Solar Cells Prepared by Electrodeposition. *Appl. Phys. Express* **2013**, *6*, 086503.
(15) Lee, Y. S.; Heo, J.; Siah, S. C.; Mailoa, J. P.; Brandt, R. E.; Kim, S. B.; Gordon, R. G.; Buonassisi, T. Ultrathin Amorphous Zinc-Tin-Oxide Buffer Layer for Enhancing Heterojunction Interface Quality in Metal-Oxide Solar Cells. *Energy Environ. Sci.* **2013**, *6*, 2112−2118.
(16) Cui, J.; Gibson, U. J. A Simple Two-Step Electrodeposition of Cu_2O/ZnO Nanopillar Solar Cells. *J. Phys. Chem. C* **2010**, *114*, 6408−6412.
(17) Musselman, K. P.; Wisnet, A.; Iza, D. C.; Hesse, H. C.; Scheu, C.; MacManus-Driscoll, J. L.; Schmidt-Mende, L. Strong Efficiency Improvements in Ultra-low-Cost Inorganic Nanowire Solar Cells. *Adv. Mater.* **2010**, *22*, E254−E258.
(18) Musselman, K. P.; Marin, A.; Wisnet, A.; Scheu, C.; MacManus-Driscoll, J. L.; Schmidt-Mende, L. A Novel Buffering Technique for Aqueous Processing of Zinc Oxide Nanostructures and Interfaces, and Corresponding Improvement of Electrodeposited ZnO-Cu_2O Photovoltaics. *Adv. Funct. Mater.* **2011**, *21*, 573−582.
(19) Chen, J.-W.; Perng, D.-C.; Fang, J.-F. Nano-Structured Cu_2O Solar Cells Fabricated on Sparse ZnO Nanorods. *Sol. Energy Mater. Sol. Cells* **2011**, *95*, 2471−2477.
(20) Luo, Y.; Wang, L.; Zou, Y.; Sheng, X.; Chang, L.; Yang, D. Electrochemically Deposited Cu_2O on TiO_2 Nanorod Arrays for Photovoltaic Application. *Electrochem. Solid-State Lett.* **2011**, *15*, H34−H36.
(21) Musselman, K. P.; Marin, A.; Schmidt-Mende, L.; MacManus-Driscoll, J. L. Incompatible Length Scales in Nanostructured Cu_2O Solar Cells. *Adv. Funct. Mater.* **2012**, *22*, 2202−2208.
(22) Yantara, N.; Mathews, N.; Jinesh, K. B.; Mulmudi, H. K.; Mhaisalkar, S. G. Modulating the Optical and Electrical Properties of All Metal Oxide Solar Cells Through Nanostructuring and Ultrathin Interfacial Layers. *Electrochim. Acta* **2012**, *85*, 486−491.
(23) Li, M.; Wu, W.; Liu, K.; Hu, G.; Xu, H. Three-Dimensional Assembly and Electrical Properties of Cu_2O/ZnO Heterojunction via an Electrochemical Superfilling Method. *Electrochim. Acta* **2012**, *71*, 100−105.
(24) Cheng, K.; Li, Q.; Meng, J.; Han, X.; Wu, Y.; Wang, S.; Qian, L.; Du, Z. Interface Engineering for Efficient Charge Collection in Cu_2O/ZnO Heterojunction Solar Cells with Ordered ZnO Cavity-Like Nanopatterns. *Sol. Energy Mater. Sol. Cells* **2013**, *116*, 120−125.
(25) Shiu, H.-Y.; Tsai, C.-M.; Chen, S.-Y.; Yew, T.-R. Solution-Processed All-Oxide Nanostructures for Heterojunction Solar Cells. *J. Mater. Chem.* **2011**, *21*, 17646−17650.
(26) Leung, S.-F.; Yu, M.; Lin, Q.; Kwon, K.; Ching, K.-L.; Gu, L.; Yu, K.; Fan, Z. Efficient Photon Capturing with Ordered Three-Dimensional Nanowell Arrays. *Nano Lett.* **2012**, *12*, 3682−3689.
(27) Deceglie, M. G.; Ferry, V. E.; Alivisatos, A. P.; Atwater, H. A. Design of Nanostructured Solar Cells Using Coupled Optical and Electrical Modeling. *Nano Lett.* **2012**, *12*, 2894−2900.
(28) Gharghi, M.; Fathi, E.; Kante, B.; Sivoththaman, S.; Zhang, X. Heterojunction Silicon Microwire Solar Cells. *Nano Lett.* **2012**, *12*, 6278−6282.
(29) Kim, D. R.; Lee, C. H.; Weisse, J. M.; Cho, I. S.; Zheng, X. Shrinking and Growing: Grain Boundary Density Reduction for Efficient Polysilicon Thin-Film Solar Cells. *Nano Lett.* **2012**, *12*, 6485−6491.
(30) Mariani, G.; Wang, Y.; Wong, P.-S.; Lech, A.; Hung, C.-H.; Shapiro, J.; Prikhodko, S.; El-Kady, M.; Kaner, R. B.; Huffaker, D. L. Three-Dimensional Core−Shell Hybrid Solar Cells via Controlled in Situ Materials Engineering. *Nano Lett.* **2012**, *12*, 3581−3586.
(31) Mariani, G.; Zhou, Z.; Scofield, A.; Huffaker, D. L. Direct-Bandgap Epitaxial Core−Multishell Nanopillar Photovoltaics Featuring Subwavelength Optical Concentrators. *Nano Lett.* **2013**, *13*, 1632−1637.
(32) Tsai, S.-H.; Chang, H.-C.; Wang, H.-H.; Chen, S.-Y.; Lin, C.-A.; Chen, S.-A.; Chueh, Y.-L.; He, J.-H. Significant Efficiency Enhancement of Hybrid Solar Cells Using Core−Shell Nanowire Geometry for Energy Harvesting. *ACS Nano* **2011**, *5*, 9501−9510.
(33) Yang, Y.; Mielczarek, K.; Aryal, M.; Zakhidov, A.; Hu, W. Nanoimprinted Polymer Solar Cell. *ACS Nano* **2012**, *6*, 2877−2892.
(34) Tétreault, N.; Arsenault, É.; Heiniger, L.-P.; Soheilnia, N.; Brillet, J.; Moehl, T.; Zakeeruddin, S.; Ozin, G. A.; Grätzel, M. High-Efficiency Dye-Sensitized Solar Cell with Three-Dimensional Photoanode. *Nano Lett.* **2011**, *11*, 4579−4584.
(35) Kim, K. S.; Song, H.; Nam, S. H.; Kim, S.-M.; Jeong, H.; Kim, W. B.; Jung, G. Y. Fabrication of an Efficient Light-Scattering Functionalized Photoanode Using Periodically Aligned ZnO Hemisphere Crystals for Dye-Sensitized Solar Cells. *Adv. Mater.* **2012**, *24*, 792−798.
(36) Liu, Y.; Turley, H. K.; Tumbleston, J. R.; Samulski, E. T.; Lopez, R. Minority Carrier Transport Length of Electrodeposited Cu_2O in ZnO/Cu_2O Heterojunction Solar Cells. *Appl. Phys. Lett.* **2011**, *98*, 162105.
(37) Musselman, K. P.; Ievskaya, Y.; MacManus-Driscoll, J. L. Modelling Charge Transport Lengths in Heterojunction Solar Cells. *Appl. Phys. Lett.* **2012**, *101*, 253503.
(38) Chen, X.; Yan, X.; Bai, Z.; Lin, P.; Shen, Y.; Zheng, X.; Feng, Y.; Zhang, Y. Facile Fabrication of Large-Scale Patterned ZnO Nanorod Arrays with Tunable Arrangement, Period and Morphology. *CrystEngComm* **2013**, *15*, 8022−8028.
(39) Chen, X.; Bai, Z.; Yan, X.; Yuan, H.; Zhang, G.; Lin, P.; Zhang, Z.; Liu, Y.; Zhang, Y. Design of Efficient Dye-Sensitized Solar Cells with Patterned ZnO-ZnS Core-Shell Nanowire Array Photoanodes. *Nanoscale* **2014**, *6*, 4691−4697.
(40) Chen, X.; Yan, X.; Bai, Z.; Shen, Y.; Wang, Z.; Dong, X.; Duan, X.; Zhang, Y. High-Throughput Fabrication of Large-Scale Highly Ordered ZnO Nanorod Arrays via Three-Beam Interference Lithography. *CrystEngComm* **2013**, *15*, 8416−8421.
(41) Golden, T. D.; Shumsky, M. G.; Zhou, Y.; VanderWerf, R. A.; Van Leeuwen, R. A.; Switzer, J. A. Electrochemical Deposition of Copper(I) Oxide Films. *Chem. Mater.* **1996**, *8*, 2499−2504.
(42) Hsu, Y.-K.; Lin, H.-H.; Wu, J.-R.; Chen, M.-H.; Chen, Y.-C.; Lin, Y.-G. Electrochemical Growth and Characterization of a p-Cu_2O Thin Film on n-ZnO Nanorods for Solar Cell application. *RSC Adv.* **2014**, *4*, 7655−7659.
(43) Lin, P.; Chen, X.; Yan, X.; Zhang, Z.; Yuan, H.; Li, P.; Zhao, Y.; Zhang, Y. Enhanced Photoresponse of Cu_2O/ZnO Heterojunction with Piezo-Modulated Interface Engineering. *Nano Res.* **2014**, *7*, 860−868.
(44) Ievskaya, Y.; Hoye, R. L. Z.; Sadhanala, A.; Musselman, K. P.; MacManus-Driscoll, J. L. Fabrication of ZnO/Cu_2O Heterojunctions in Atmospheric Conditions: Improved Interface Quality and Solar Cell Performance. *Sol. Energy Mater. Sol. Cells* **2014**, DOI: 10.1016/j.solmat.2014.09.018.

DOI: 10.1021/am507836v
ACS Appl. Mater. Interfaces 2015, 7, 3216−3223